

OPTIMISATION OF SINGLE TRANSITION CROSS POLARISATION

Emanuel Winterfors

Reviewed by István Furó

Department of Physical Chemistry, KTH

Supervised by Geoffrey Bodenhausen

Département de Chimie, Ecole Normale Supérieure
24 rue Lhomond, 75231 Paris cedex 05, France

Table of content

FUNDAMENTAL CONCEPTS AND DEFINITIONS	1
BASIC QUANTUM PHYSICS.....	1
<i>Wave functions</i>	1
<i>Choice of base</i>	1
<i>Operators</i>	1
<i>Expectation values</i>	1
<i>The Schrödinger equation</i>	2
QUANTUM STATISTICS	2
<i>Ensemble</i>	2
<i>Density operator</i>	2
<i>Orthonormal bases in Liouville space</i>	3
<i>Single transition operators</i>	3
<i>The Liouville-von Neumann equation</i>	4
<i>Hamiltonian super operator</i>	4
RELAXATION THEORY	5
<i>The master equation</i>	5
<i>Solving the master equation</i>	5
CONVENTIONAL CROSS POLARISATION	8
SOLID STATE CROSS POLARISATION.....	8
LIQUID STATE CROSS POLARISATION	8
THE HARTMAN-HAHN CONDITION	9
HARD PULSE ALTERNATIVES	9
SINGLE TRANSITION CROSS POLARISATION.....	10
MODEL OF THE CONSIDERED SYSTEM.....	10
COORDINATE FRAME FOR A TIME INDEPENDENT HAMILTONIAN	10
CHARACTERISTICS OF SOLUTIONS FOR ON- AND OFF-RESONANCE TRANSFER	11
EIGENVALUE REQUIREMENTS FOR OPTIMAL TRANSFER	13
<i>Hamiltonian and Liouvillian eigenfrequency theory</i>	13
<i>Eigenfrequencies of the transfer Hamiltonian</i>	14
<i>Eigenfrequencies of the transfer Liouvillian</i>	14
TRANSFER FIELD STRENGTH FOR OPTIMAL TRANSFER	15
IRRADIATION DURATION FOR OPTIMAL TRANSFER	16
HARD PULSE ALTERNATIVES	16

APPLICATION: SEPARATING TRANSFER OF ST COHERENCES	18
EXPERIMENTAL ASPECTS	18
<i>Field matching</i>	18
<i>The use of gradients</i>	18
<i>Creation of single transition coherences</i>	19
<i>Full pulse sequence used in experiments</i>	20
APPLICATION TO SLOWLY RELAXING MOLECULE (TBOC-GLYCINE).....	21
<i>Simulations</i>	21
<i>Experiments</i>	22
APPLICATION TO FAST RELAXING MOLECULE (VISCOUS SUCROSE)	23
<i>Preparation and characterisation of the sample</i>	24
<i>Compensating for peak broadening</i>	24
<i>Simulations</i>	26
<i>Experiments</i>	27
SUMMARY AND CONCLUSIONS	29
REFERENCES.....	30
TABLES.....	31
FIGURES.....	31
ABBREVIATIONS	31
SYMBOLS.....	32
INDEX	33

Abstract

A single transition separating transfer of coherence between two scalar-coupled nuclei of spin $\frac{1}{2}$ is shown to be obtainable in a time of $\frac{3}{\sqrt{7}} \times J$ s by radiofrequency irradiation of amplitude $2 \times J/3$ Hz at the eigenfrequencies of one single transition of each nucleus. This result represents a further development of the Single Transition Cross Polarisation (STCP) method, recently invented by Ferrage, Eykyn and Bodenhausen (2000), which produces the same transfer using a considerably longer irradiation time. The results are derived analytically using a novel method of transfer characterisation by the eigenfrequencies of the transferring Liouvillian, thereafter verified experimentally and by numerical simulation.

Fundamental concepts and definitions

Basic quantum physics

Wave functions

According to the postulates of quantum mechanics, any system can be completely described by a wave function, which is a complex-valued function over all degrees of freedom of the system.

$$\Psi : \mathbf{D} \rightarrow \mathbf{C}, (x_1, x_2, x_3, \dots) \in \mathbf{D} \quad (1)$$

where the set \mathbf{D} on which λ is defined may consist of an arbitrary number of variables (for a particle, this may be coordinates in time and space).

Choice of base

Considering ψ a member of a linear set of functions (for instance \mathbf{L}^2) it may be decomposed into a linear combination of other functions of the same set. It is often useful to express wave functions in terms of an orthogonal series of base functions, which may be finite or infinite depending of the nature of the definition set of the functions. In the case of a finite series, all functions of the space can be represented by vectors. There usually exist several different alternatives for orthogonal base to express a wave function in, providing different advantages.

Operators

Every measurable quantity may be represented by an operator, mapping the space of wave functions onto itself.

$$\hat{\mathbf{A}} : \mathbf{L} \rightarrow \mathbf{L}, \text{ where } \Psi \in \mathbf{L} \quad (2)$$

The outcome of such a measurement is however constrained to one of the eigenvalues of the operator, that is, it has to fulfil the equation

$$\lambda \Psi = \hat{\mathbf{A}} \Psi \quad (3)$$

where λ is an eigenvalue of operator $\hat{\mathbf{A}}$ and Ψ the corresponding eigenfunction.

Expectation values

In quantum physics, the scalar product between two elements of a vector space (e.g. \mathbf{L}) is usually written $\langle \Psi | \Phi \rangle$ and may be defined¹

$$\langle \Psi | \Phi \rangle = \int_{x \in D} \Psi^*(x) \Phi(x) dx \quad (4)$$

where * denotes complex conjugate.

¹ Gasiorowicz, p45

To be in line with this notation, one usually writes a wave function Ψ as $|\Psi\rangle$ and its complex conjugate Ψ^* as $\langle\Psi|$. This is commonly referred to as ‘Dirac notation’ and will be used throughout this and the following chapters.

An expectation value of an observable \mathbf{A} on a certain system represented by Ψ is the average value that an infinite number of measurements would yield. In accordance with the definitions made above, it may be defined as

$$\langle \hat{A} \rangle = \langle \Psi | \hat{A} | \Psi \rangle \quad (5)$$

The Schrödinger equation

The time evolution of a quantum system is defined by the time-dependent Schrödinger equation:

$$i \frac{\hbar}{2\pi} \frac{\partial}{\partial t} \Psi = \hat{H} \Psi \quad (6)$$

where \hat{H} is the Hamiltonian representing the total energy of the system, \hbar is the Planck constant and $i^2 = -1$. In quantum descriptions of NMR, the term is often dropped (or – more strictly – included in the Hamiltonian), to yield a somewhat more compact notation:

$$\frac{\partial}{\partial t} \Psi = -i2\pi \hat{H} \Psi \quad (7)$$

which will be used throughout this presentation. This way, the Hamiltonian is expressed in Hz, an energy unit that is easy to relate to the radio frequency radiation emitted by spin systems.

Quantum statistics

Ensemble

An ensemble may be defined as a (presumably very large) number of quantum systems, identical except for that any member may be in any quantum state.

Density operator

When dealing with an ensemble of identical systems, it is convenient to represent it using only enough information to calculate the evolution of the expectation value of an observable on the ensemble. Given the observable \hat{A} on the ensemble of quantum systems $|\Psi_n\rangle$, its expectation value is written:

$$\langle \hat{A} \rangle = \sum_{\forall n} \langle \Psi_n | \hat{A} | \Psi_n \rangle \quad (8)$$

Reformulating (8) with the aim of separating observable and wave functions, the same expectation value may be expressed

$$\langle \hat{A} \rangle = \text{tr} \left(\hat{A} \left| \sum_{\forall n} |\Psi_n\rangle\langle\Psi_n| \right. \right) \quad (9)$$

It is now possible to define a new operator, collecting the contributions to any observable expectation value from all (possibly infinite) members of the ensemble:

$$\hat{\sigma} = \sum_{\forall n} |\Psi_n\rangle\langle\Psi_n| \quad (10)$$

In accordance with (9), the expectation value of any observable \hat{A} the ensemble can be written:

$$\langle \hat{A} \rangle = \text{tr}(\hat{A} | \hat{\sigma}) \quad (11)$$

Orthonormal bases in Liouville space

Just as wave functions, density operators may be defined as belonging to a linear vector space (usually referred to as Liouville space) and may be decomposed into linear combinations of elements of this space. If the wave functions on which an operator operates can be represented by vectors, the operator may be represented by a matrix thus fitting into the definitions of linear algebra.

Single transition operators

Considering a system of two spin $1/2$, it is possible to span the entire sixteen-dimensional Liouville space by single transition operators¹

$$\begin{aligned} \hat{\mathbf{I}}_d^{(1,2)} &= \hat{\mathbf{I}}^{\alpha} \hat{\mathbf{S}}_d & \hat{\mathbf{I}}_d^{(3,4)} &= \hat{\mathbf{I}}^{\beta} \hat{\mathbf{S}}_d & \hat{\mathbf{I}}^{\alpha} &= \frac{1}{2} \hat{\mathbf{I}} + \hat{\mathbf{I}}_z \\ & & & & \hat{\mathbf{I}}^{\beta} &= \frac{1}{2} \hat{\mathbf{I}} - \hat{\mathbf{I}}_z \\ & & & & \hat{\mathbf{I}} &= \text{identity operator} \end{aligned} \quad d \in \{x, y, z\} \quad (12)$$

To span the complete Liouville space, four additional operators are needed:

$$\begin{aligned} \hat{\mathbf{I}}_x^{(1,4)} &= \hat{\mathbf{I}}_x \hat{\mathbf{S}}_x - \hat{\mathbf{I}}_y \hat{\mathbf{S}}_y & \hat{\mathbf{I}}_x^{(1,4)} &= \hat{\mathbf{I}}_x \hat{\mathbf{S}}_y + \hat{\mathbf{I}}_y \hat{\mathbf{S}}_x \\ \hat{\mathbf{I}}_x^{(2,3)} &= \hat{\mathbf{I}}_x \hat{\mathbf{S}}_x + \hat{\mathbf{I}}_y \hat{\mathbf{S}}_y & \hat{\mathbf{I}}_y^{(2,3)} &= \hat{\mathbf{I}}_y \hat{\mathbf{S}}_x - \hat{\mathbf{I}}_x \hat{\mathbf{S}}_y \end{aligned} \quad (13)$$

Worth noting is that there are no “z-direction” operators corresponding to the latter four, and that they do not correspond to any detectable magnetisation. Further, there is a constraint on the sum of the four “z-direction” operators reducing the dimensionality of the subspace in which the operator evolves to fifteen, instead of sixteen dimensions.

The commutation rules for the ST operators are as follows:

¹ Ernst et al. p 36

$$\begin{aligned}
[\hat{I}_x^{(r,s)}, \hat{I}_y^{(r,s)}] &= i\hat{I}_z^{(r,s)} && \text{as for cyclic permutations thereof.} \\
[\hat{I}_x^{(r,s)}, \hat{I}_x^{(t,s)}] &= [\hat{I}_y^{(r,s)}, \hat{I}_y^{(t,s)}] = -[\hat{I}_x^{(r,t)}, \hat{I}_z^{(s,t)}] = \frac{i}{2}\hat{I}_y^{(r,t)} \\
[\hat{I}_x^{(r,t)}, \hat{I}_y^{(s,t)}] &= -[\hat{I}_y^{(r,s)}, \hat{I}_z^{(t,s)}] = \frac{i}{2}\hat{I}_x^{(r,s)} && r, s, t, u \text{ are permutations of } \{1,2,3,4\} \\
[\hat{I}_a^{(r,s)}, \hat{I}_b^{(t,u)}] &= [\hat{I}_z^{(r,s)}, \hat{I}_z^{(t,s)}] = 0 && a, b \in \{x, y, z\}
\end{aligned} \tag{14}$$

The Liouville-von Neumann equation

From the Schrödinger equation (7), one can easily derive an equivalent equation for an ensemble of quantum systems represented by a density operator. This equation is called the Liouville-von Neumann equation (LvN equation) and is usually written

$$\frac{d}{dt}\hat{\sigma}(t) = -2\pi i[\hat{H}(t), \hat{\sigma}(t)] \tag{15}$$

where the commutator brackets are defined as

$$[\hat{A}, \hat{B}] = \hat{A}\hat{B} - \hat{B}\hat{A} \tag{16}$$

A symbolic solution to (15) may be written

$$\hat{\sigma}(t) = e^{-2\pi i \int \hat{H}(t) dt} \hat{\sigma}_{t=0} e^{2\pi i \int \hat{H}(t) dt} \tag{17}$$

where the two exponential functions represents a time dependent, unitary transformation of the initial state. In general this transformation is too complex to be calculated analytically. In NMR however, the density operator usually has rather few dimensions and the Hamiltonian may in addition often be considered constant for a finite number of time intervals. This permits the calculation of rather simple analytical solutions.

If the Hamiltonian is independent of time, (17) simplifies to

$$\hat{\sigma}(t) = e^{-2\pi i t \hat{H}} \hat{\sigma}_{t=0} e^{2\pi i t \hat{H}} \tag{18}$$

Here the exponential functions can (at least in finite-dimensional cases) easily be calculated by choosing a suitable base that renders the Hamiltonian diagonal.

Hamiltonian super operator

As an alternative to commutator formalism, one may instead view the commutation of the Hamiltonian with any other operator as a mapping of a Liouville space onto itself. Such a transformation may be represented by a super operator and is defined in two alternative forms (using operator and tensor formalism) below.

$$\hat{H} : \hat{A} \rightarrow [\hat{H}, \hat{A}] \tag{19}$$

$$H_{pqkl} A_{kl} = (H_{ki \in jl} - H_{kj \in il}) A_{kl}$$

Having defined the Hamiltonian super operator \hat{H} , it is possible to simplify the LvN equation (15) to a form analogous to differential equations:

$$\frac{d}{dt} \hat{\sigma}(t) = -2\pi i \hat{H} \hat{\sigma}(t) \quad (20)$$

A symbolic solution equivalent to (17) then reads:

$$\hat{\sigma}(t) = e^{-2\pi i \int \hat{H}(t) dt} \hat{\sigma}_{t=0} \quad (21)$$

as for the simpler case of a time-independent Hamiltonian:

$$\hat{\sigma}(t) = e^{-2\pi i t \hat{H}} \hat{\sigma}_{t=0} \quad (22)$$

Relaxation theory

The master equation

Including only the nuclear spins in a description of a quantum system – as in equation (10) – works well on a time scale of one or a few milliseconds (in liquids). However, for the evolution of the system over a longer period of time, the approximation breaks down since the spin system will evolve towards thermal equilibrium with its surroundings (often referred to as ‘the lattice’). This is equivalent with a loss of coherence and is mediated by random interactions affecting only a few ensemble members at a time. These interactions are therefore impossible to include in a Hamiltonian universal for the whole ensemble as used in (7), (15), (20) etc. Instead, each member of the ensemble would have to be treated as a part of a quantum system of interactions between first interactions between all members of the ensemble and second their interactions with the surroundings.

Such a system is however too complex to fully represent in any theoretical model. Instead an approximation can be made, provided the number of ensemble members is high and their interactions very fast in comparison with the period one wishes to describe.

Then, in accordance with the laws of statistical mechanics, the loss of coherence is exponential by nature and may therefore be described by a mere decay rate correction term to the LvN equation, expressed in super operator form (20):

$$\frac{d}{dt} \hat{\sigma}(t) = 2\pi i \hat{H} \hat{\sigma}(t) - 2\pi \hat{R}(\hat{\sigma}(t) - \hat{\sigma}_{eq}) \quad (23)$$

The decay rates represented by \hat{R} , the relaxation super operator, are proportional to the deviation of $\hat{\sigma}(t)$ from its (non-irradiated) state of thermal equilibrium, denoted $\hat{\sigma}_{eq}$.

Solving the master equation

By including both the Hamiltonian commutator and the relaxation super operator in one single super operator, often called the Liouvillian:

$$\hat{\Gamma} = i\hat{H} - \hat{R} \quad (24)$$

as well as noting that $d(\hat{\Gamma}^{-1} \hat{R} \hat{\sigma}_{eq}) / dt = 0$, one might rewrite the master equation (23) as:

$$\frac{d}{dt} \left(\hat{\sigma}(t) + \hat{\Gamma}^{-1} \hat{R} \hat{\sigma}_{eq} \right) = 2\pi \hat{\Gamma} \left(\hat{\sigma}(t) + \hat{\Gamma}^{-1} \hat{R} \hat{\sigma}_{eq} \right) \quad (25)$$

This is (provided the Hamiltonian is time independent) nothing but a system of ordinary differential equations of the first degree, which can be solved in the same way as equation (22):

$$\hat{\sigma}(t) + \hat{\Gamma}^{-1} \hat{R} \hat{\sigma}_{eq} = e^{2\pi \hat{\Gamma} t} \left(\hat{\sigma}_0 + \hat{\Gamma}^{-1} \hat{R} \hat{\sigma}_{eq} \right) \quad (26)$$

For a more compact notation, two additional definitions are often made:¹

$$\hat{\sigma}_{ss} = -\hat{\Gamma}^{-1} \hat{R} \hat{\sigma}_{eq} \Leftrightarrow \hat{\sigma}_{eq} = -\hat{R}^{-1} \hat{\Gamma} \hat{\sigma}_{ss}, \quad \hat{\sigma}'(t) = \hat{\sigma}(t) - \hat{\sigma}_{ss} \quad (27)$$

allowing for (26) to be written:

$$\hat{\sigma}'(t) = e^{2\pi \hat{\Gamma} t} \hat{\sigma}'_0 \quad (28)$$

¹ Ernst et al. p. 16

Conventional cross polarisation

Solid state cross polarisation

The technique of cross polarisation was originally introduced by S. R. Hartmann and E. L. Hahn in the early sixties as a way of transferring coherence between nuclei in solid state NMR¹. It consists of continuously irradiating the two nuclei between which a transfer is to take place at their respective Larmor frequencies. If there are dipolar interactions between the two nuclei (that may be of the same or of different nuclear species) an interchange of coherent magnetisation will then take place that may be used to transfer coherence from one nucleus to the other.

Liquid state cross polarisation

The use of cross polarisation in liquid state NMR was not investigated until in the late seventies². The experimental methods are quite the same as in solid state NMR: the two nuclei between which a transfer of coherence is to take place are irradiated at their respective larmor frequencies for a limited period of time. The coherence transfer is however mediated by scalar coupling (that is through chemical bonds) instead of through dipolar interactions directly between spatially close nuclei.

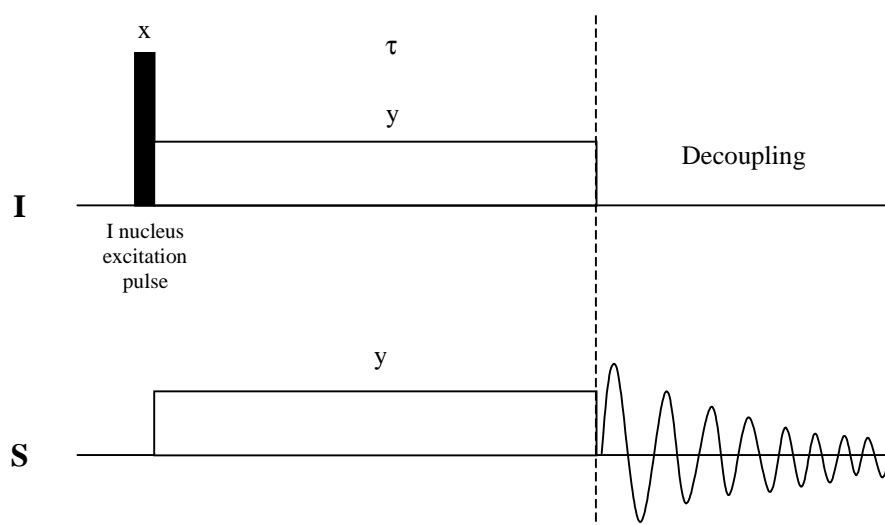


Figure 1: Liquid state CP sequence

The use of the method is by far not as widespread as its solid state counterpart, mainly due to its high sensitivity to violation of the Hartman-Hahn (HH) condition, which is described below. Good HH calibration is often unobtainable for the full sample volume because of inhomogeneities in the RF excitation fields. This is in turn due to the fact that the excitation coils are optimised for detection rather than for producing homogeneous fields³.

¹ Hartmann, Hahn

² Maudsley et al.

³ Levitt, p. 30

The Hartman-Hahn condition

A common feature of both solid and liquid state CP is the way the irradiation field strengths must be adapted to each other for the transfer to be efficient. In terms of their rotating action on their respective nuclear spin, both fields must be of equal strength (expressed in Hz, or equivalently). This condition bears the name of the CP inventors¹ and may be explained by Liouvillian degeneracy theory, which is however only outlined in this review.

Hard pulse alternatives

The CP method achieves a transfer of in-phase coherence from one nucleus to another. This may also be accomplished by employing sequences of hard pulses, spaced by periods of free precession under the J-coupling Hamiltonian. The latter method acts on a very broad range of chemical shifts of both heteronuclei, whereas CP has a high frequency selectivity.

The most basic hard pulse sequence for coherence transfer through J-coupling is the INEPT pulse sequence. It transfers – just like CP – only in-phase coherence.

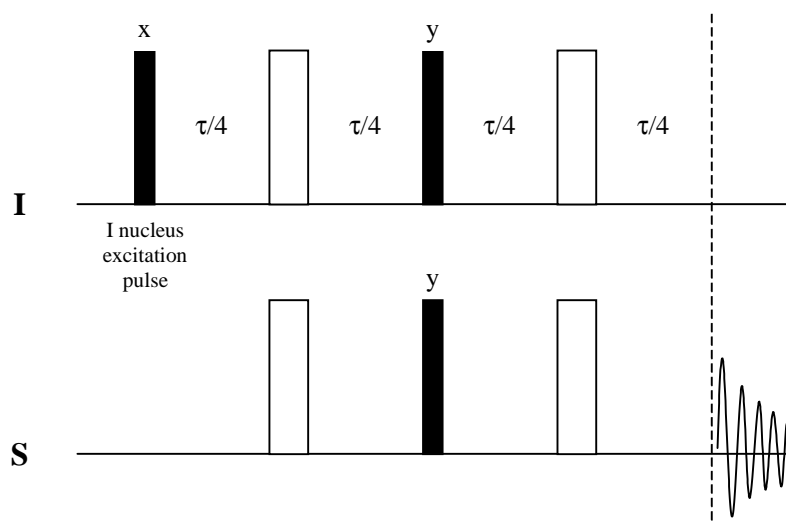


Figure 2: INEPT pulse sequence for coherence transfer in J-coupled heteronuclear pairs

¹ Hartmann, Hahn

Single transition cross polarisation

A J-coupling between two nuclei gives (as described previously) rise to two energy eigenstates on each nucleus. In terms of density operators, they will correspond to single transition coherence operators that with an appropriate rotational transformation of the coordinate frame can be rendered independent of time.

Single transition cross polarisation is a recent development of the original liquid state cross polarisation method. Just as for conventional cross polarisation, the aim is to transfer coherence from nuclei with one particular precession frequency to nuclei with another. The difference lies in the way that single transition coherences are transferred. Where conventional CP will transfer only in-phase coherence, which is equivalent with a particular linear combination of the two ST coherences, STCP will transfer each single transition to only one single transition of the target nucleus, respectively.

Model of the considered system

Single transition cross polarisation (STCP) is a phenomenon that takes place in scalar-coupled heteronuclear pairs, just as conventional liquid-state cross polarisation. To model such a system, it is sufficient to regard the evolution of a 4×4 density matrix that yields a sixteen-dimensional Liouvillian space.

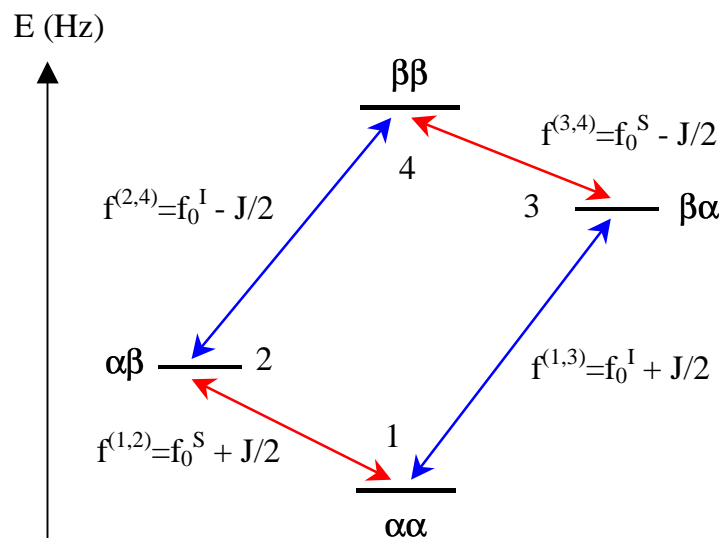


Figure 3: Quantum states and transitions of a J-coupled pair of nuclei with spin $\frac{1}{2}$

Coordinate frame for a time independent Hamiltonian

Considering a J-coupled pair of nuclei (below denoted I and S), the Hamiltonian expressed in a frame rotating with the Larmor frequencies of each nucleus consist only of one term containing the scalar coupling.

$$\hat{H}_J^{I,S} = J \hat{I}_z \hat{S}_z \quad (29)$$

In order to include terms for RF fields irradiating on the exact frequencies of one of the single transition coherences of each nucleus in a time-independent manner, a transformation

consisting of a rotation with half the frequency of the J-coupling on each nucleus is necessary, yielding a rotating frame Hamiltonian:

$$\hat{H}_J^{r.f.} = J\hat{I}_z\hat{S}_z + \frac{J}{2}\hat{I}_z + \frac{J}{2}\hat{S}_z \quad (30)$$

It is now possible to form the total Hamiltonian during the irradiation period by adding the terms for the irradiation intensities, Ω_I and Ω_S .

$$\hat{H}_{tot}^{r.f.} = J\hat{I}_z\hat{S}_z + \frac{J}{2}\hat{I}_z + \frac{J}{2}\hat{S}_z + \Omega_I\hat{I}_x + \Omega_S\hat{S}_x \quad (31)$$

To simplify the analytical treatment of the LvN equation containing this Hamiltonian, one might make a restriction to the case where $\Omega_I = \Omega_S$ in other words when the Harman-Hahn condition is fulfilled. Introducing the variable w , defined as:

$$w = \frac{\sqrt{\Omega_I^2 + \Omega_S^2}}{J} = \sqrt{2} \frac{\Omega}{J} \quad (32)$$

it is possible to write the whole Hamiltonian as proportional to J . This means that expressed in this way, the J-coupling strength affects only the speed or time scale of the evolution of the system during the irradiation period and *no other* of its dynamic properties.

$$\hat{H} = J\left(\hat{I}_z\hat{S}_z + \frac{\hat{I}_z + \hat{S}_z}{2} + w\frac{\hat{I}_x + \hat{S}_x}{\sqrt{2}}\right) \quad (33)$$

Characteristics of solutions for on- and off-resonance transfer

In order to have a STCP, there are two basic requirements that have to be fulfilled at the end of the irradiation period. First, in order to be an efficient CP transfer, as much as possible of the magnetisation on the source nucleus should be transferred to the target nucleus. Second, all magnetisation transferred from one of the single transitions of the source nucleus should end up on one of the two STs of the target nucleus in order for the transfer to be ST separating.

From this, two conditions may be set up for the on- and off-resonance transfers respectively to be STCP transfers:

Beginning with all magnetisation on one single transition of the source nucleus, (i) more than 90% of it shall be on the target transition and (ii) less than 0.5% of it on the undesired transition of the target nucleus by the end of the transfer.

The development of the system during the irradiation period is governed by equation (20):

$$\frac{d}{dt}\hat{\sigma}(t) = 2\pi i\hat{H}\hat{\sigma}(t) \text{ – the LvN equation in super operator form – which according to (22) has}$$

a solution $\hat{\sigma}(t) = e^{2\pi i\hat{H}t}\hat{\sigma}_{t=0}$, since the Hamiltonian is time independent. To find which combinations of transfer field strengths (w) and transfer durations (t) fulfils the requirements, solutions of the were calculated for a range of field strenghts $0 < wJ < J$, marking the areas that match each of the requirements. The time evolution during the on-resonance transfer was

calculated with $\hat{\sigma}_{t=0} = S_x^{(1,2)}$ and the off-resonance with $\hat{\sigma}_{t=0} = S_x^{(3,4)}$, both using the same Hamiltonian.

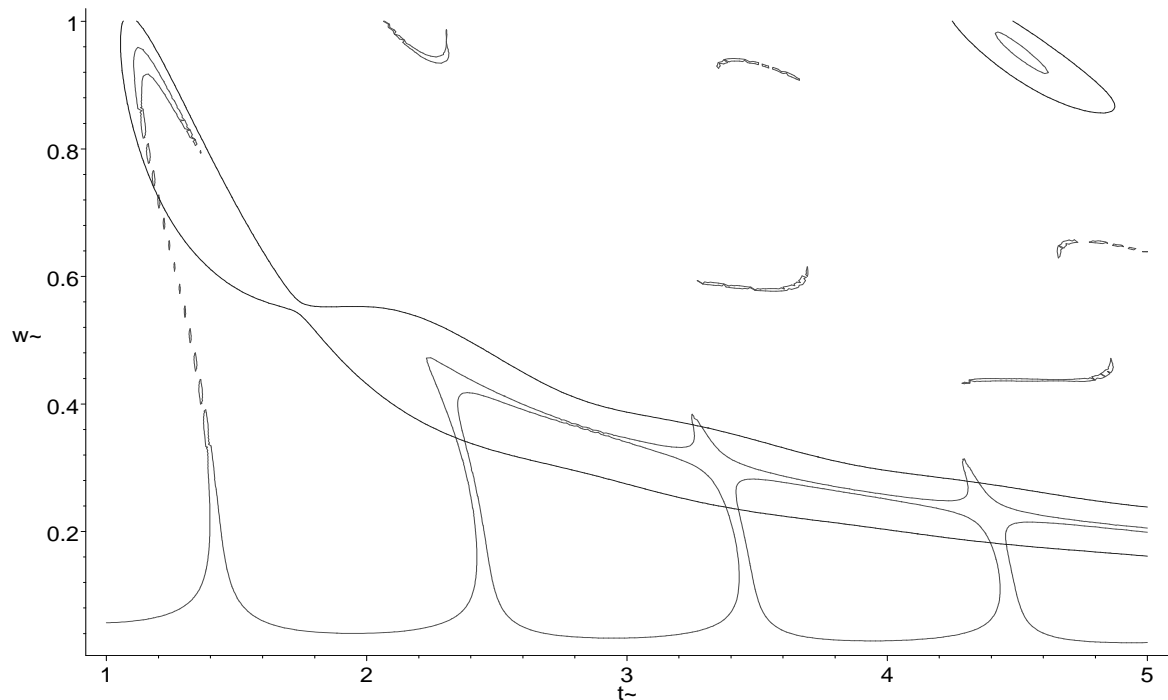


Figure 4: Encircled areas fulfilling conditions for more than 90% magnetisation at desired ST (thicker line) and less than 0.5% at undesired ST (thinner line) using on-resonance transfer.

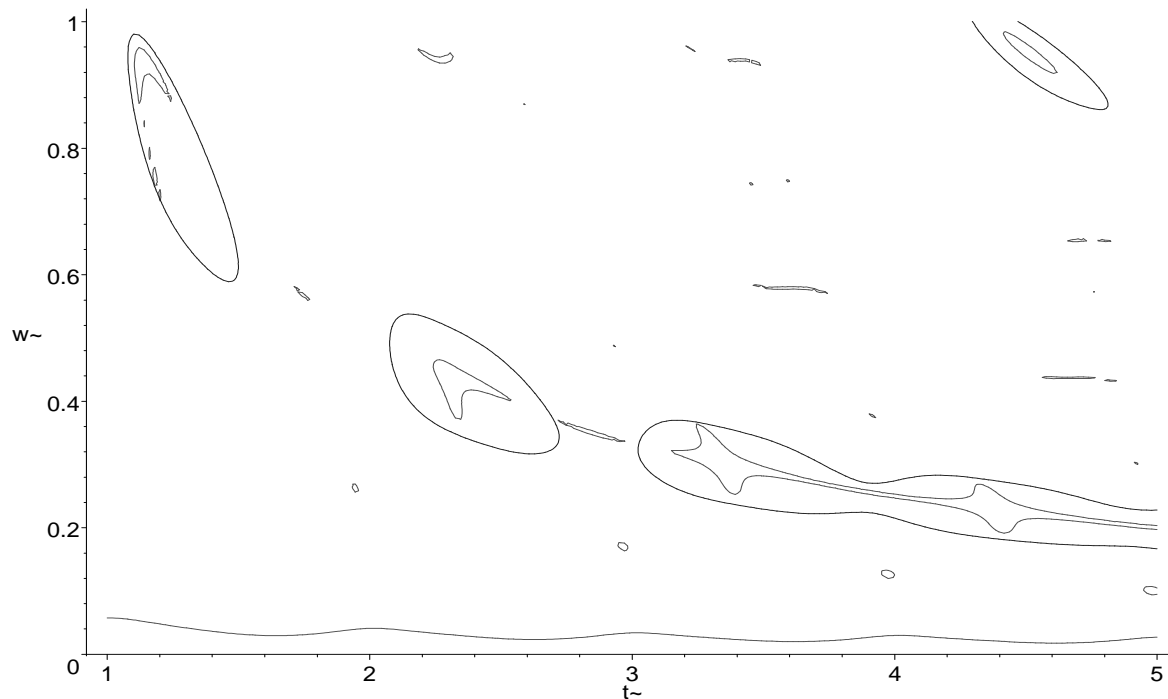


Figure 5: Encircled areas fulfilling conditions for more than 90% magnetisation at desired ST (thicker line) and less than 0.5% at undesired ST (thinner line) using off-resonance transfer.

Looking for areas encircled by both a thin and a thicker line, one will find that ideal STCP properties for both the on and off-resonance transfers may be found around the following pairs of intensity and duration of the irradiation fields:

Area (from left to right)	Field strength (wJ) in Hz	Irradiation duration (t) in seconds
(i)	0.94 J	1.15 J ⁻¹
(ii)	0.44 J	2.3 J ⁻¹
(iii)	0.32 J	3.35 J ⁻¹
(iv)	0.24 J	4.4 J ⁻¹

Figure 6: Table of values of field strength and duration for optimal STCP transfer

It is worth noting that the condition of having a negligible unwanted transfer is better fulfilled in between the latter three points than between the first and second. This implies that the sensitivity to field strength or irradiation time miscalibration is lower for lower field strengths. An increased transfer time does however also mean decrease in signal strength due to relaxation.

Eigenvalue requirements for optimal transfer

To find a simple explanation to this result by studying the analytical solution is difficult, since both eigenvalues and eigenvectors of matrices – even as small as 4×4 – generally take a complicated form. A hint of when the right requirements may be fulfilled can however be obtained by just studying the eigenvalues of the Liouvillian.

Hamiltonian and Liouvillian eigenfrequency theory

An eigenvalue λ_i of a given operator \hat{H} is by definition any value that fulfils the equation

$$\hat{H}\Psi_i = \lambda_i \Psi_i \quad i \in \{1..n\} \quad (34)$$

where n is the dimension of the function space and Ψ_i the eigenfunction corresponding to λ_i . A linear operator representing a one-to-one mapping from one vector space of dimension n into another will have $n \times n$ eigenvalues:

$$\hat{H}\hat{\rho}_{ij} = \kappa_{ij} \hat{\rho}_{ij} \quad i, j \in \{1..n\} \quad (35)$$

As a consequence of its definition (22), the $n \times n$ eigenfrequencies κ_{ij} of the Hamiltonian super operator may be calculated from those of the Hamiltonian:

$$\kappa_{ij} = \lambda_i - \lambda_j \quad i, j \in \{1..n\} \quad (36)$$

Out of these, n will be equal to zero (where $i=j$) and the other will form $(n^2-n)/2$ pairs of positive and negative real eigenvalues.

Eigenfrequencies of the transfer Hamiltonian

Normalised by the inverse of the coupling constant J and expressed in eigenbase of $\hat{H}^{l.f.}$, the transferring Hamiltonian – defined in equation (33) – may be written:

$$J^{-1} \hat{H} = \frac{1}{4} \begin{bmatrix} 3 & \sqrt{2}w & \sqrt{2}w & 0 \\ \sqrt{2}w & -1 & 0 & \sqrt{2}w \\ \sqrt{2}w & 0 & -1 & \sqrt{2}w \\ 0 & \sqrt{2}w & \sqrt{2}w & -1 \end{bmatrix} \quad (37)$$

Since the Hamiltonian is a hermitian operator, its matrix representation is self-adjoint and has real eigenvalues. They represent the eigenfrequencies of the normalised Hamiltonian and will depend on w in a non-trivial way that is expressed analytically below.

$$\begin{aligned} \frac{\lambda_1}{J} &= \frac{1}{12} - \frac{\cos u}{3\sqrt{2}}x + \frac{\sin u}{\sqrt{6}}x, & \frac{\lambda_2}{J} &= \frac{1}{12} + \frac{\sqrt{2} \cos u}{3}x, \\ \frac{\lambda_3}{J} &= \frac{1}{12} - \frac{\cos u}{3\sqrt{2}}x - \frac{\sin u}{\sqrt{6}}x, & \frac{\lambda_4}{J} &= -\frac{1}{4} \end{aligned} \quad (38)$$

where

$$u = \frac{1}{3} \arctan\left(\frac{9w\sqrt{16+13w^2+8w^4}}{\sqrt{3}(8-9w^2)}\right) \text{ and } x = \sqrt{2+3w^2} \quad (39)$$

Eigenfrequencies of the transfer Liouvillian

For a system of two spin $\frac{1}{2}$ (for which $n=4$), this gives six non-zero eigenvalue pairs, which may be expressed:

$$\begin{aligned} \frac{\kappa_{12}}{J} &= -\frac{\kappa_{21}}{J} = \frac{1}{3} - \frac{\cos u}{3\sqrt{2}}x + \frac{\sin u}{\sqrt{6}}x \text{ (i)}, & \frac{\kappa_{13}}{J} &= -\frac{\kappa_{31}}{J} = -\frac{\sin u}{\sqrt{6}}x + \frac{\cos u}{\sqrt{2}}x \text{ (ii)}, \\ \frac{\kappa_{14}}{J} &= -\frac{\kappa_{41}}{J} = \frac{1}{3} + \frac{\sqrt{2} \cos u}{3}x \text{ (iii)}, & \frac{\kappa_{23}}{J} &= -\frac{\kappa_{32}}{J} = \frac{1}{3} - \frac{\cos u}{3\sqrt{2}}x - \frac{\sin u}{\sqrt{6}}x \text{ (iv)}, \\ \frac{\kappa_{24}}{J} &= -\frac{\kappa_{42}}{J} = -\frac{\sin u}{\sqrt{6}}x - \frac{\cos u}{\sqrt{2}}x \text{ (v)}, & \frac{\kappa_{43}}{J} &= -\frac{\kappa_{34}}{J} = -2\frac{\sin u}{\sqrt{6}}x \text{ (vi)} \end{aligned} \quad (40)$$

where u and x are defined as in (39).

Plotting the absolute values of these gives the following image of their dependence of the Ω_{tot}/J ratio, w :

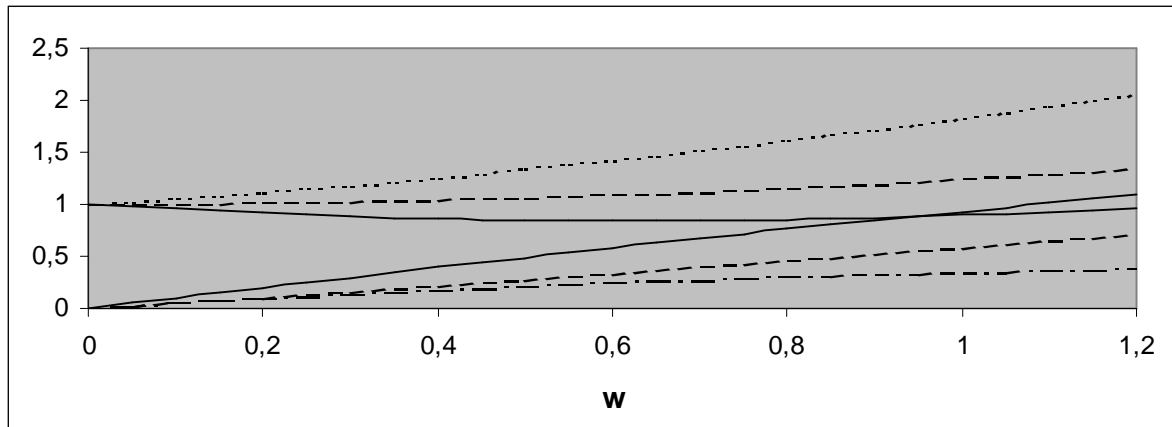


Figure 7: Liouvillian eigenfrequency ($1=1 \times J$) dependence of w (Ω_{tot}/J ratio)

At zero field strength, all eigenfrequencies are either equal to zero or J , just as one might have expected. With increasing field strength, eigenvalues begin to diverge, first forming two groups of three around 0 and J respectively. At $w=0.5$ they are more or less evenly distributed between 0 and $1.5 \times J$ and at $w=0.94$ an intersection occurs between the absolute values of eigenvalues (ii) and (vi). This intersection corresponds to area (i) of Figure 6 which is where conditions for a optimal STCP transfer are fulfilled. In analogy with this, areas (ii), (iii) and (iv) in the same figure will correspond to intersections of multiples of the eigenvalues in equations (40).

Transfer field strength for optimal transfer

Setting eigenvalue (ii) + eigenvalue (vi) = 0 yields the equation:

$$\frac{1}{\sqrt{2}}(\cos u - \sqrt{3} \sin u)x = 0 \quad (41)$$

Searching for a solution with only the expression inside the parenthesis equal to zero gives the standard trigonometric equation with a lowest solution of $u=\pi/6$.

$$\cos u = \sqrt{3} \sin u \Rightarrow u = \frac{\pi}{6} \quad (42)$$

According to equations (39), $\tan(3u)$ is equal to a polynomial fraction of w . But since $\lim_{u \rightarrow \pi/2} \tan u = \infty$, it is required for the nominator, $\sqrt{3}(8-9w^2)$, to have a root there. This gives the following important requirement for the total field strength of an optimal transfer:

$$\sqrt{3}(8-9w^2) = 0 \Rightarrow w = \pm \frac{2}{3}\sqrt{2} \quad (43)$$

With the Hartmann-Hahn condition fulfilled, this means that the two irradiation field strengths should be two thirds of the J -coupling strength.

$$\Omega_I = \Omega_S = \frac{2}{3}J \quad (44)$$

Irradiation duration for optimal transfer

At a field intensity of $wJ = 2\sqrt{2}J/3 = \sqrt{8/9}J$, the eigenvalues of the transferring Liouvillian takes a simple form:

$$\begin{aligned} \frac{\kappa_{12}}{J} = -\frac{\kappa_{21}}{J} = \frac{2\sqrt{7}}{3} \quad (\text{i}), & & \frac{\kappa_{13}}{J} = -\frac{\kappa_{31}}{J} = \frac{\sqrt{7}}{3} \quad (\text{ii}), \\ \frac{\kappa_{14}}{J} = -\frac{\kappa_{41}}{J} = \frac{1}{3} \quad (\text{iii}), & & \frac{\kappa_{23}}{J} = -\frac{\kappa_{32}}{J} = \frac{\sqrt{7}}{3} \quad (\text{iv}), \\ \frac{\kappa_{24}}{J} = -\frac{\kappa_{42}}{J} = \frac{\sqrt{7}}{3} + \frac{1}{3} \quad (\text{v}), & & \frac{\kappa_{43}}{J} = -\frac{\kappa_{34}}{J} = \frac{\sqrt{7}}{3} - \frac{1}{3} \quad (\text{vi}) \end{aligned} \quad (45)$$

It is the two equal eigenfrequencies (ii) and (iv) that will be (equally) responsible for the undesired coherence transfer. For an optimal coherence transfer, their contributions should cancel out. This may happen only when the complex value of the eigenvector propagator $e^{-2\pi i \kappa t}$ is purely imaginary. In that case, if $-2\pi i \kappa_{23} t_{\text{tot}} = -\sqrt{7} 2\pi i J t_{\text{tot}}/3 = -2\pi i$, the total irradiation time t_{tot} must be:

$$t_{\text{tot}} = \frac{3}{\sqrt{7}J} \quad (46)$$

in order to obtain a single transition separating coherence transfer. It will thus transfer coherence from the irradiated single transition of the source nucleus to the irradiated ST of the target nucleus, as well as from the non-irradiated ST of the source nucleus to the non-irradiated ST of the target nucleus.

Hard pulse alternatives

If the aim is to obtain a ST separating coherence transfer that will act on J-coupled pairs in a broad range of chemical shifts, many different variants of hard pulse sequences can be used. In analogy with the INEPT sequence (Figure 2, p 9) for interchanging either the in-phase *or* the anti-phase coherences of two J-coupled nuclei, there exist pulse sequences that interchange both in- and anti-phase coherence, thereby also interchanging the single transition coherences.

One such sequence that transfers both single transition coherences from one nucleus (denoted I) to another (denoted S) is shown below. The time τ denotes $1/J$, where J is the coupling strength in Hz. As a consequence of the symmetry between the pulses on each of the nuclei, the transfer will work in both ways, interchanging their magnetisation.

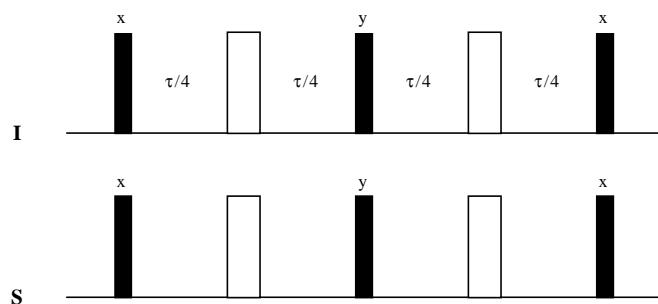


Figure 8: Pulse sequence for single transition separating coherence transfer

Application: separating transfer of ST coherences

The general aim of the experiments undertaken here is to study the evolution of different single transition coherences during the ST irradiation period. This serves primarily two purposes: first to test the correctness of the theoretical model by comparison with the numerically calculated results, second to see whether the STCP method really does obtain a one-to-one ST coherence transfer and to what disturbing factors this property may be sensitive.

Experimental aspects

Field matching

In order to obtain a good Hartmann-Hahn match of the two irradiation fields, a standard method of calibration was used. It consist of two sequential CP sequences, transferring magnetisation from proton to the target nucleus, de-phasing the magnetisation of non-irradiated or non-J-coupled nuclei with a shaped gradient pulse, finally transferring the remaining magnetisation back for detection on the proton.

By varying one of the irradiation fields over a range of amplitudes while keeping the other constant, the optimal amplitude ratio is easily found, corresponding to the combination giving the strongest detected signal.

The use of gradients

Magnetic field gradients have a wide range of uses in NMR. They are of crucial importance to magnetic resonance imaging, where they form the basic principle for discriminating one point in space from another. In NMR spectroscopy of homogeneous samples (where no such distinction is necessary) they also have important uses.

The basic idea behind the use of gradients is very simple. It uses the fact that the precession frequency of a nuclear spin is directly proportional to the magnetic field strength. Applying a gradient in that field will thus introduce a difference in precession frequency along the spatial dimension of the gradient. This will cause nuclei of identical molecules to emit radiation at different frequencies during the time the gradient is applied – which is the principle used for imaging. The nuclei experiencing a strong magnetic field will ‘move ahead’ of those experiencing a weaker one, causing coherently precessing nuclei to be constantly more and more de-phased during the gradient field.

The most important application to NMR spectroscopy is to use this de-phasing property of gradients to reduce or completely eliminate unwanted signals. This is achieved by putting the magnetisation that one wishes to detect in a state where it is not precessing with time. In a J-coupled pair of nuclei for instance, this may be along I_z , S_z or $I_z S_z$. Applying a magnetic field gradient for a limited time – usually around one millisecond – will then de-phase all coherently precessing magnetisation, rendering it undetectable. Then, the magnetisation of interest can be turned into detectable coherences through any suitable pulse sequence.

Water suppression

One of the most common situations in which suppression of all signals arising from a particular molecule is when a larger molecule of interest is dissolved in a solvent consisting of small molecules (i.e. water). In that case, the signal produced by the solvent will be so much

stronger than the signal of interest that it may render it undetectable (or at least leave less dynamic range of signal intensity for the signal of interest) or conceal possibly important parts of it.

There exists a multitude of techniques of how to separate the solvent signal from the one of interest¹. The technique used in the experiments performed for this review is based on pulsed gradients, along the principles described in the previous section.

Creation of single transition coherences

In order to enable the study of how single transition coherences are transferred from one nucleus to another, it is useful to be able to create a state where all magnetisation is along one of the two single transitions of a nucleus.

The ideal state would be to be able to go from having all magnetisation along I_z to having it along only one of the single transitions, i.e. $I_x + 2I_xS_z$. Unfortunately, the two single transition coherences are separated in the sense that their magnetisation may be interchanged, but not merged into one single coherence precessing with one frequency.

Excitation of only one of the two single transition coherences is possible in a number of different ways. One is a simple pulse sequence designed by the author, consisting of only two $\pi/4$ pulses on the same nucleus with x- and y-phase respectively, separated by a total delay of $\tau/2$ ($\tau=1/J$) and possibly a π -pulse on each of the nuclei to refocus chemical shifts.

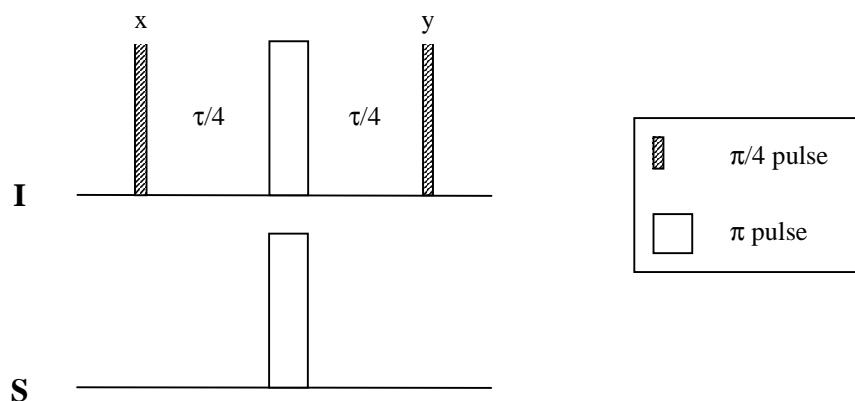


Figure 9: Pulse sequence for creation of single transition coherence

Exciting one of the single transitions, the pulse sequence leaves the other one along the z-direction thus with a potential of interacting with latter parts of a longer series of pulses.

The use of a gradient does however allow for the complete elimination of this possible disturbance. Adding a gradient pulse after the pulse sequence described above dephases the excited single transition coherence, after which the remaining the remaining magnetisation can then be turned into a pure single transition coherence by a simple $\pi/2$ pulse.

¹ Wider et al

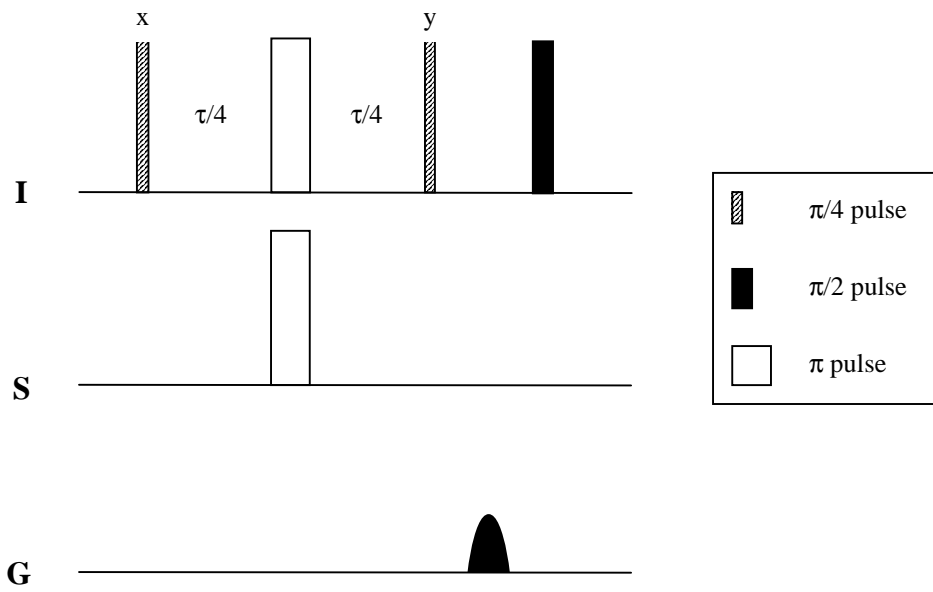


Figure 10: Pulse sequence for creation of single transition coherence eliminating longitudinal magnetisation

Full pulse sequence used in experiments

To verify the ST separating transferring property of the optimised STCP method, a very straightforward method was used. By creating one pure single transition coherence on the S nucleus, transferring it by STCP yields the exact ratio between the resulting transferred ST coherences on the I nucleus, hopefully 1:0.

For increased selectivity and signal strength, conventional CP sequence was used to transfer magnetisation from the I nucleus to the S nucleus. The magnetisation on the J-coupled S nuclei was then turned into Z-direction magnetisation by a $\pi/2$ pulse on the S channel, followed by two pulsed gradients and a $\pi/2$ I channel pulse to de-phase the magnetisation of all other nuclei.

Employing a combination of $\pi/4$ and π pulses as well as a pulsed gradient (as described in Figure 10, p 20) a pure ST coherence was then created on the S nucleus, followed by a STCP transfer for which the duration, t_{tot} , was varied to enable the study of the time evolution during the transfer.

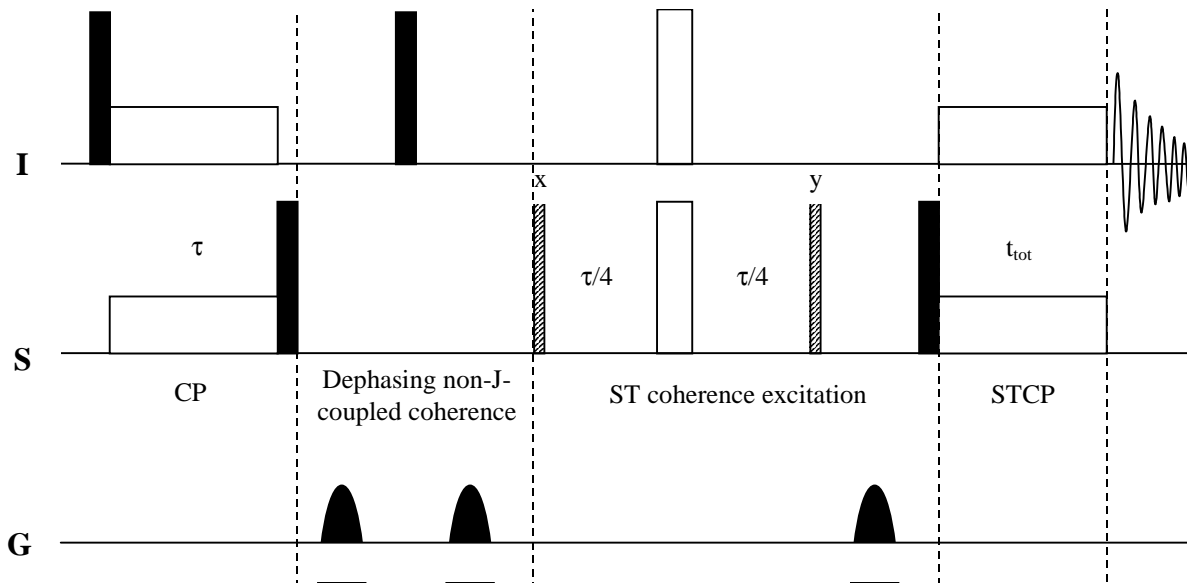


Figure 11: Pulse sequence used in experiments

Application to slowly relaxing molecule (tboc-glycine)

In order to test the general applicability and detect possible practical difficulties of the method, it was first applied to a simple and well-known molecule with almost negligible transverse relaxation rates: tboc-glycine.

Simulations

To calculate the time evolution of a STCP transfer on this small, slowly relaxing molecule, a numerical approach implemented in C++ invoking the Gamma subroutine package¹ was used. Since phenomena due to relaxation are negligible on the timescale of interest, relaxation was completely ignored. The reason for not choosing a fully analytical approach was only the convenience of using a method consistent with the ones used for simulations taking relaxation into account.

For a J-coupled ^1H - ^{15}N pair with a coupling strength $J=94$ Hz in the molecule, the time evolution of the ‘goal’ transition $I^{(2,4)}$ as well as the ‘undesired’ transition $I^{(1,3)}$ was calculated for a transfer field strength of 62 Hz (equals a 89 Hz total transfer field).

This gives a Hamiltonian $\hat{H}_{tot}^{r.f.} = 94(\hat{I}_z \hat{S}_z + (\hat{I}_z - \hat{S}_z)/2 + 2(\hat{I}_x + \hat{S}_x)/3)$ which was set to act *on-resonance* on – that is irradiating the eigenfrequency of – an initial state $\hat{\sigma}_{t=0} = \hat{S}_x^{(1,2)}$, yielding the following time evolution of the absolute amount of the STs on the target proton (percentage relative to maximal transferred coherence):

¹ Smith et al.

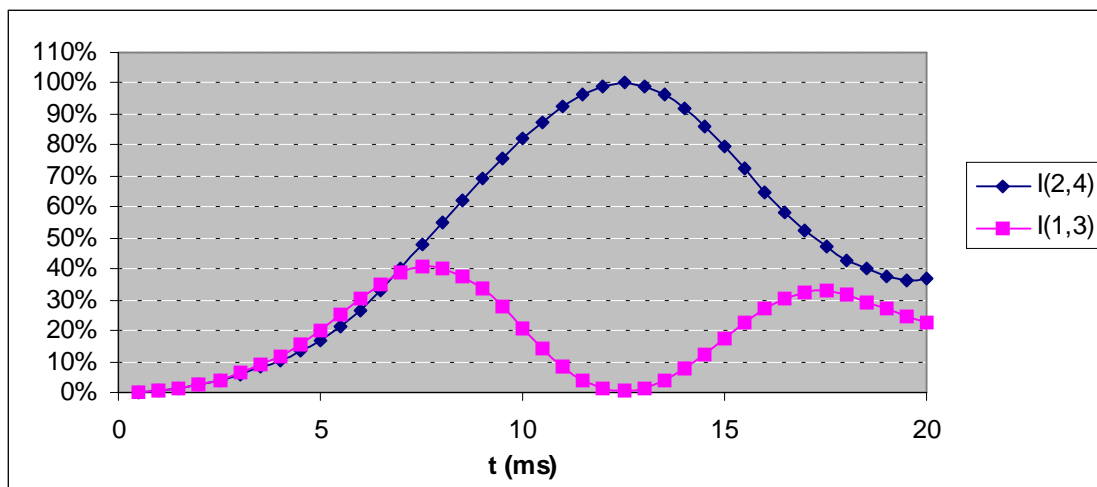


Figure 12: Simulated evolution of on-resonance STCP transfer neglecting relaxation

The transfer evolution of the other, *off-resonance* ST coherence on the ^{15}N nucleus was calculated in the same manner, but using an initial state $\hat{\sigma}_{t=0} = \hat{S}_x^{(3,4)}$, which should be transferred to the $\hat{I}^{(2,4)}$ ST coherence.

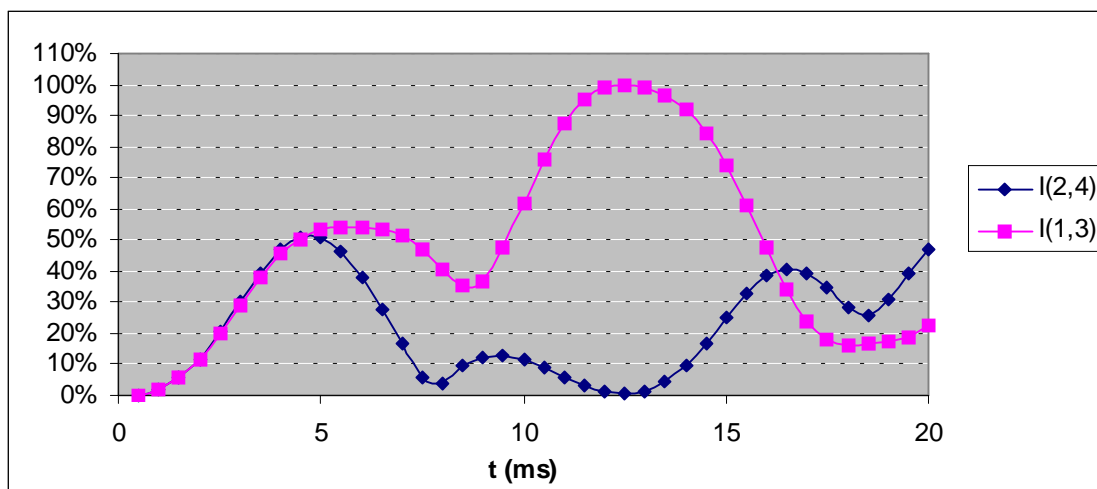


Figure 13: Simulated evolution of off-resonance STCP transfer neglecting relaxation

For the transfer of both coherences, there is an irradiation duration $t_{tot} = 3/(\sqrt{7} \times 94) = 12$ ms (46) for which the transfer to the ‘undesired’ transition is eliminated. Since the transfer will constitute a linear transformation of the initial state density operator, the one-to-one transferring property will include any combination of the two ST coherences on the ^{15}N nucleus.

Experiments

To determine the exact frequencies of the single transitions of the ^1H and ^{15}N nuclei, a HSQC experiment was performed (without any decoupling). The middle frequency in-between the doublet of a 94 Hz J-coupled ^{15}N - ^1H pair was measured in both frequency dimensions to be

used for the initial conventional CP transfer, and the highest frequency of the doublets for the following STCP transfer.

Applying the pulse sequence in Figure 11, the absolute amplitude of the ST coherences on the proton for a range of durations of the STCP irradiation period, to yield the following result for the coherence transferred *on-resonance*:

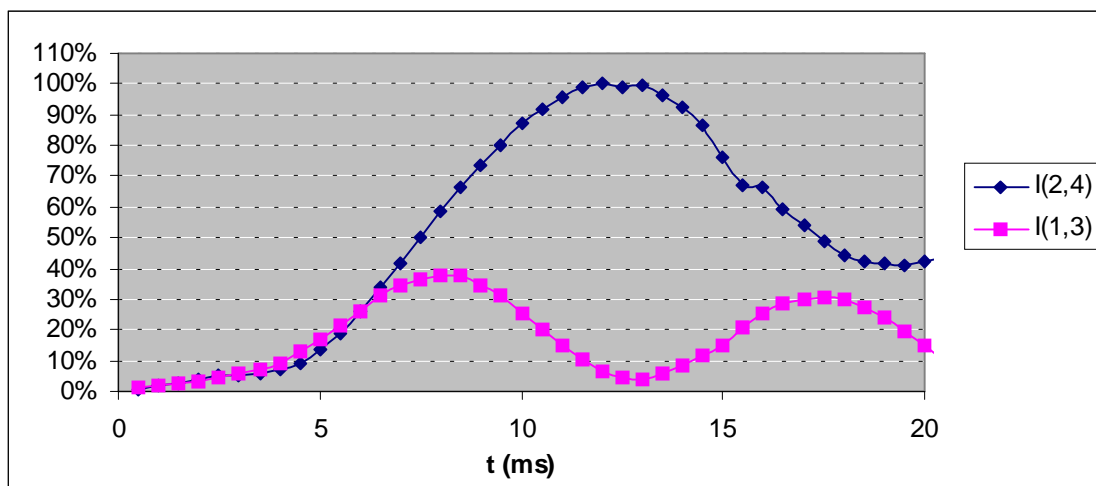


Figure 14: Measured evolution of on-resonance STCP transfer in tboc-glycine

The same procedure was repeated transferring a ST coherence off-resonance, again producing results agreeing with the simulations.

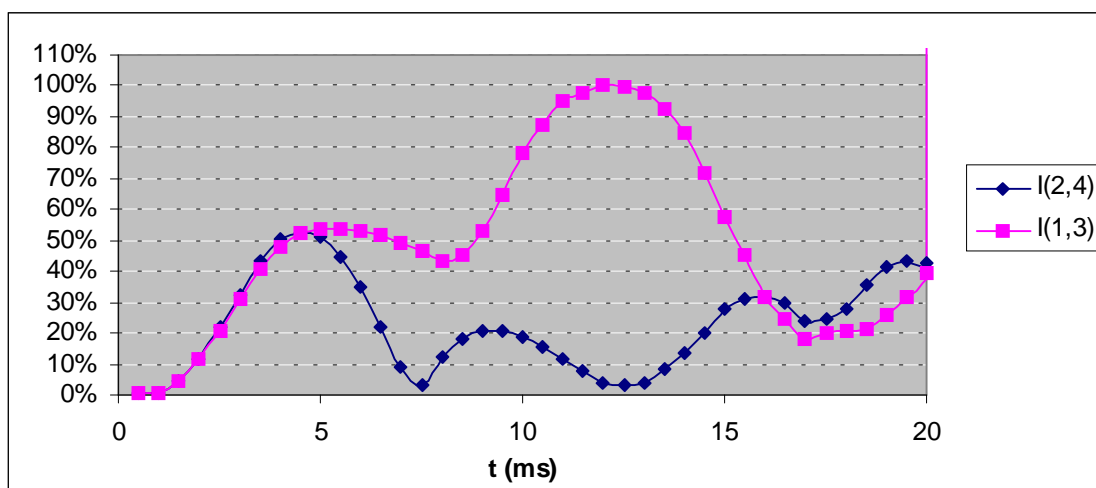


Figure 15: Measured evolution of off-resonance STCP transfer in tboc-glycine

Application to fast relaxing molecule (viscous sucrose)

Since the total transfer time of an optimised STCP experiment is comparable to the one of conventional CP, it should be possible to apply it to the study of ‘fast relaxing’ molecules, such as large proteins. To prove this, the method was applied to natural-abundance ^1H - ^{13}C pairs in a viscous sugar solution with relaxation times of around 10 ms.

Preparation and characterisation of the sample

The sample was prepared by mixing 0.703 g sucrose with 0.360 g deuterated water at a temperature of 60 °C in order to form a 66% close-to-saturated sucrose solution, without risking polymerisation to take place¹.

The transverse relaxation rate of the protons was measured by a standard CPMG experiment, yielding monoexponentially decaying intensities of all peaks originating from the sugar molecule. At a temperature of 300 K, a relaxation rate of 103 s⁻¹ was measured – equivalent to a transverse relaxation time of 9.7 ms.

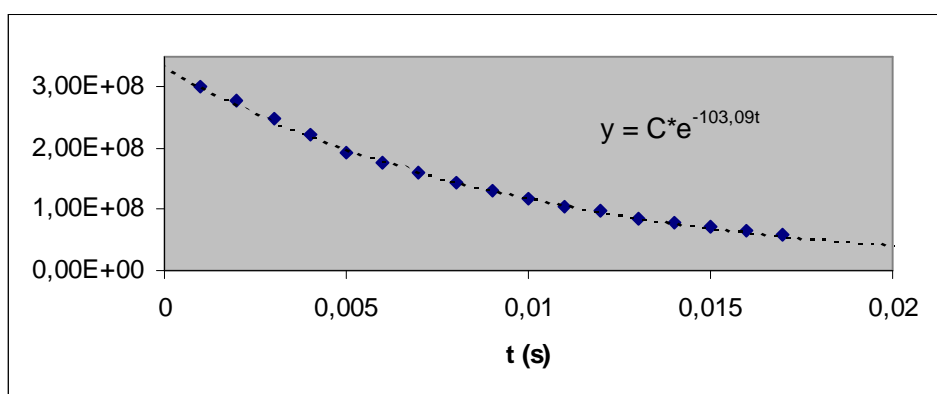


Figure 16: Measured proton peak intensity as a function of delay before detection

As for the tboc-glycine sample, the frequencies and coupling constant of a selected J-coupled heteronuclear pair was measured using an un-decoupled variant of the standard HSQC experiment.

The J-coupling of the selected pair was measured to be 175 Hz.

Compensating for peak broadening

The high relaxation rate of the protons will yield a fast-decaying signal, for which – if originating from a frequency f_0 – the time dependence can be expressed:

$$g(t) = e^{(2\pi f_0 i - \frac{1}{T_2})t} \quad (47)$$

Transforming into frequency space (using fourier transform over the positive time axis) still using Hz as frequency unit, yields a simple complex-valued fractional expression reaching its maximum at $f=f_0$

$$G(f) = \int_{t=0}^{\infty} g(t)e^{-2\pi i f t} dt = \frac{1}{\frac{1}{T_2} + 2\pi i (f - f_0)} \quad (48)$$

¹ Morgan, Jeffrey, p 3473

Considering a peak at $f_0=0$ with a transverse relaxation time of 9.7 ms, this expression takes the form:

$$G(f) = \frac{1}{103 + 2\pi if} \quad (49)$$

The absolute value of this expression at 175 Hz offset is 9.33% of its maximal peak value. Measuring intensities of single transition peaks of J-coupled pairs in fast-relaxing molecules like this one, this implies that there will be a considerable overlap between even quite distant peaks. If there are also uncoupled nuclei at the same chemical shift as the coupled ones (as is the case here), this third peak will further interfere with the other two.

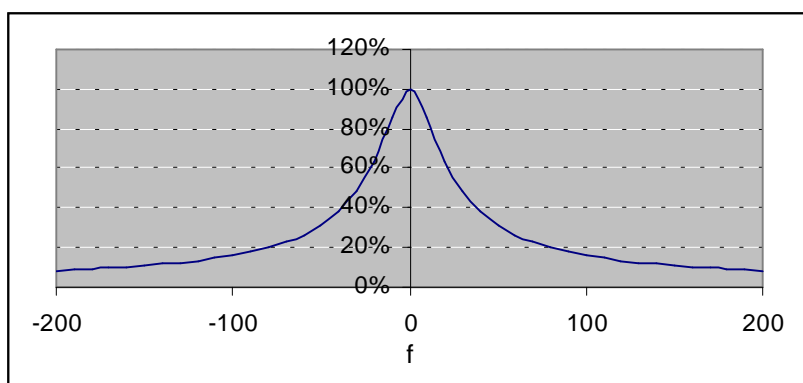


Figure 17: Calculated magnitude spectrum of exponential decay with 9.7 ms relaxation time

If, however, the precession frequency of the nucleus of interest is known, one can easily compensate for the overlap of the three peaks, provided the signals from which they origin can be considered monoexponential. Since the signal is nothing but a linear combination of all its components, the ‘true’ peak intensities can be calculated just by solving the linear system of equations formed by the contributions of each of the three peaks at each of the three frequencies:

$$\begin{aligned} I_1^{measured} &= I_1^{real} G(0) + I_2^{real} G(J/2) + I_3^{real} G(J) \\ I_2^{measured} &= I_1^{real} G(-J/2) + I_2^{real} G(0) + I_3^{real} G(J/2) \\ I_3^{measured} &= I_1^{real} G(-J) + I_2^{real} G(-J/2) + I_3^{real} G(0) \end{aligned} \quad (50)$$

where I_n indicates the complex peak intensities and J the scalar coupling strength.

In matrix algebra this may be written

$$\bar{I}^{measured} = [G] \bar{I}^{real} \quad (51)$$

with the solution:

$$\bar{I}^{real} = [G]^{-1} \bar{I}^{measured} \quad (52)$$

Thus, the ‘true’ peak intensities for three overlapping peaks (with the same relaxation time) on a complex-valued spectrum may be calculated just by multiplying all the measured intensities with an inverse of this G matrix calculated ‘once and for all’ in advance.

Simulations

Again using the Gamma package of C++ subroutines, a prediction of the time evolution of the amplitude of the two single transitions of the target nucleus was calculated using numerical diagonalisation of the transferring Liouvillian.

To set the elements of the relaxation super operator, a phenomenological approach was used, first assuming that any cross relaxation or correlation rate is negligible. The remaining auto-decay rates of all ST coherences defined in equations (12) and (13) was set either according to a CPMG measurement (as for the four observable ST coherences on proton and ^{13}C) or by extrapolation of the relaxation rates of similar molecules under similar conditions.

For the on-resonance transfer, an evolution very similar to that of a non-relaxing system should be obtained, except for a considerable decrease in signal strength and an incomplete elimination of the transfer to the undesired transition. This relaxation-induced imperfection of the ST separating property of the transfer is however merely around 5% of the desired coherence amplitude at the duration of optimal transfer $t_{tot} = 3/(\sqrt{7} \times 170) = 6.7$ ms, which will permit measurements of sufficient precision in virtually all practical applications.

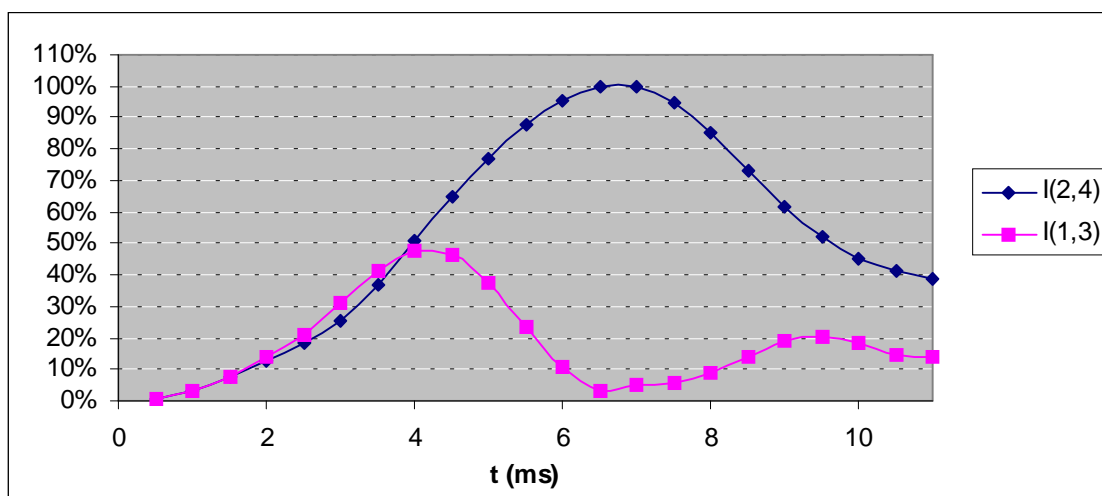


Figure 18: Simulated evolution of on-resonance STCP transfer in sucrose

The time evolution of the by *off-resonance* transferred ST coherence differs somewhat more from its non-relaxing counterpart, but the amount of coherence transferred to the undesired ST still stays around 5% the amplitude of the desired ST coherence.

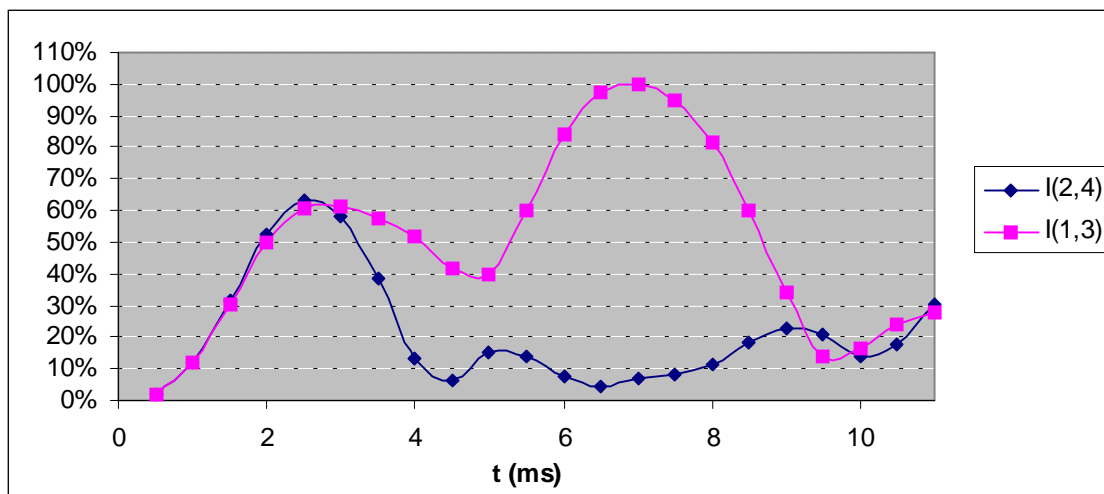


Figure 19: Simulated evolution of off-resonance STCP transfer in sucrose

Experiments

Applying CP pulses to a solution as viscous as 66% sucrose imposed an experimental difficulty that had not been foreseen. The viscosity causes significant distortion in both the B_0 and B_1 field, causing parts of the sample to be irradiated by fields at mismatched frequency or with intensities not fulfilling the HH condition.

These effects add together to increase the amount of undesired coherence in the signal and – somewhat more confusingly – causes it to seemingly evolve slower than expected from the coupling strength. A transfer time that produces below 15% of undesired ST coherence may be picked, but it corresponds a $t_{tot} = 8$ ms rather than the theoretical value of $t_{tot} = 6.7$ ms.

The general appearance of the evolution of the ST coherence transferred *on-resonance* shares many features with the result of the simulation, but differs significantly in optimal transfer time.

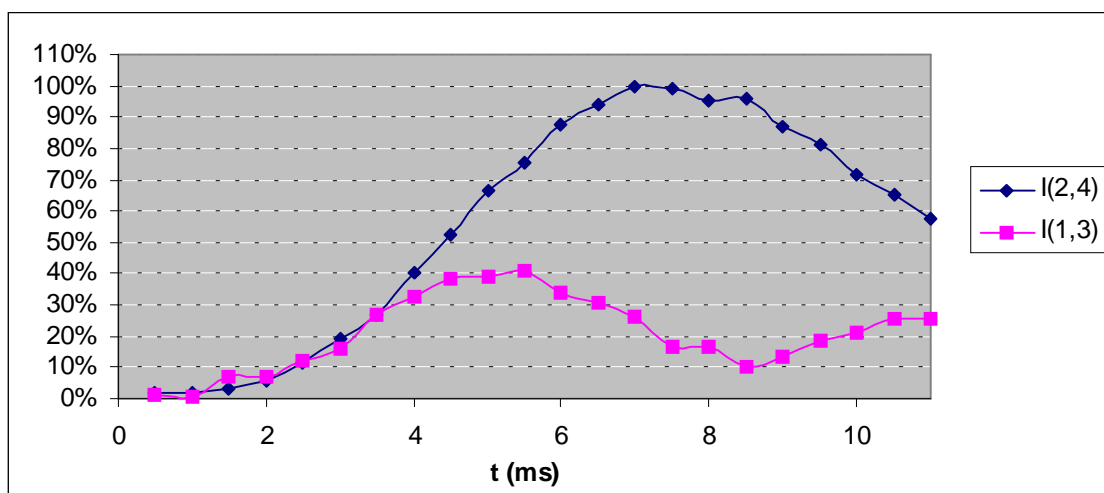


Figure 20: Measured evolution of on-resonance STCP transfer in sucrose

For the ST coherence transferred off-resonance the differences from the simulations prevail: a optimal transfer time can be found creating much less than 15% undesired ST coherence compared to the desired one, but it is significantly longer than the theoretical value.

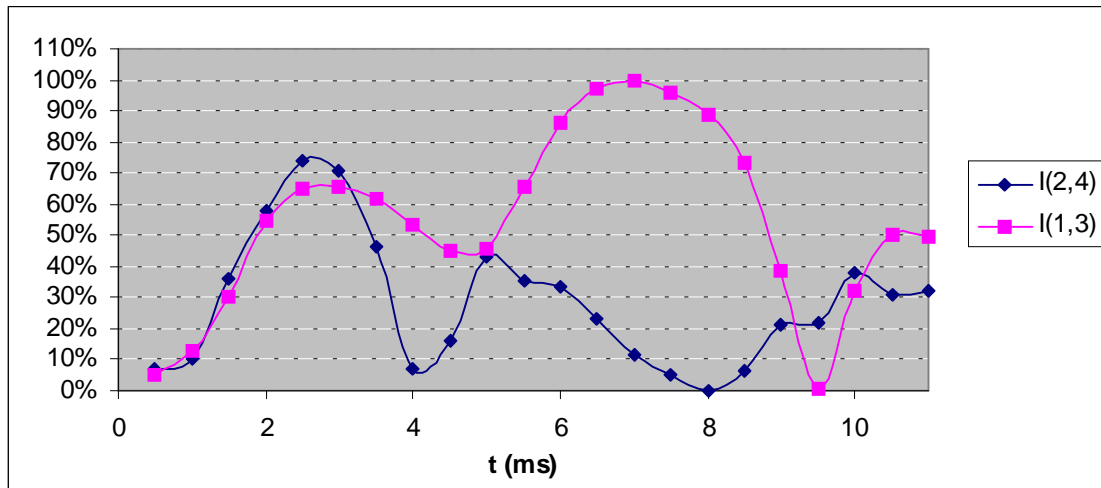


Figure 21: Measured evolution of off-resonance STCP transfer in sucrose

Summary and conclusions

In the theoretical section, the method of Single Transition Cross Polarisation (STCP) is investigated analytically, without invoking the secular approximation of the transferring Hamiltonian that has been used in previous theoretical descriptions. Relaxation is however neglected. Through this approach, it is demonstrated that it is possible to reduce the transfer time for the method down to about one-third of that proposed in the original article¹.

To explain this result, a novel analytical tool is introduced for the analysis of quantum coherence transfer, based on the eigenfrequencies of the transferring Liouvillian. Using this tool, the ideal intensity of the irradiation fields is calculated to be $\Omega=2J/3$ Hz for both nuclei and the total transfer time $t_{\text{tot}}=3/(\sqrt{7}J)$ s. Both expressions differ from previous estimates based on the secular approximation.

The experimental section contains a precise verification of the predicted properties of the optimised STCP method applied to a slow-relaxing molecule (tbc-glycine), at the same time directly verifying the single transition separation property of the transfer. The possibility of obtaining a single transition separating transfer in a fast-relaxing molecule (viscous sucrose with a T_2 of 10 ms) is also demonstrated, although experimental difficulties due to the viscosity of the sample introduce certain differences from the simulated time evolution of the system. This suggests that application to an isotope-enriched large proteins of comparable relaxation rates would be preferable to completely verify the applicability of the method.

¹ Ferrage et al.

References

- Chiarparin et al. E. Chiarparin, P. Pelupessy and G. Bodenhausen: *Selective cross-polarization in solution state NMR*. Molecular Physics, vol.95, no.5, 10 Dec. 1998, pp.759-67
- Ernst et al. R. R. Ernst, G. Bodenhausen and A. Wokaun: *Principles of nuclear magnetic resonance in one and two dimensions* Oxford University Press 1987
- Ferrage et al. F. Ferrage, T. R. Eykyn and G. Bodenhausen *Coherence transfer by single-transition cross-polarisation: Quantitation of cross-correlation effects in nuclear magnetic resonance*, Journal of Chemical Physics vol. 113, no. 3, 15 July 2000
- Gasiorowicz S. Gasiorowicz: *Quantum physics*, John Wiley & sons (second edition) 1996
- Hartmann, Hahn S. R. Hartmann and E. L. Hahn: *Phys Rev* 128, 2042 (1962)
- Levitt M. H. Levitt: *Heteronuclear cross polarisation in liquid-state nuclear magnetic resonance: Mismatch compensation and relaxation behaviour*, J. Chem. Phys. 95 (1) Jan. 1991, p 30-38
- Maudsley et al. A. A. Maudsley, L. Müller and R. R. Ernst, J. Magn. Res. 28, 463 (1977)
- Mehring et al. M. Mehring, E. K. Wolff and M. E. Stoll: *Exploration of the eight-dimensional spin space of a spin-1 particle by NMR*, Journal of Magnetic Resonance vol.37, no.3, 15 Feb. 1980 p.475-95
- Morgan, Jeffrey G. R. Morgan and K. R. Jeffery: *A study of the molecular motion in glucose/water mixtures using deuterium nuclear magnetic resonance*, J. Chem. Phys Vol 110, no 7, 15 Feb 1999
- Smith et al. S. A. Smith, T. O. Levante, B. H. Meier and R. R. Ernst: *Computer simulations in magnetic resonance. An object-oriented programming approach*, Journal of Magnetic Resonance, Series A. vol.106, no.1; Jan. 1994; p.75-105
- Wider et al. G. Wider, R. V. Hosur and K. Wuthrich: *Suppression of the solvent resonance in 2D NMR spectra of proteins in H₂O solution*. Journal of Magnetic Resonance, vol.52, no.1, March 1983, p.130-5

Tables

Figures

FIGURE 1: LIQUID STATE CP SEQUENCE	8
FIGURE 2: INEPT PULSE SEQUENCE FOR COHERENCE TRANSFER IN J-COUPLED HETERONUCLEAR PAIRS	9
FIGURE 3: QUANTUM STATES AND TRANSITIONS OF A J-COUPLED PAIR OF NUCLEI WITH SPIN $\frac{1}{2}$	10
FIGURE 4: ENCIRCLED AREAS FULFILLING CONDITIONS FOR MORE THAN 90% MAGNETISATION AT DESIRED ST (THICKER LINE) AND LESS THAN 0.5% AT UNDESIRED ST (THINNER LINE) USING ON-RESONANCE TRANSFER	12
FIGURE 5: ENCIRCLED AREAS FULFILLING CONDITIONS FOR MORE THAN 90% MAGNETISATION AT DESIRED ST (THICKER LINE) AND LESS THAN 0.5% AT UNDESIRED ST (THINNER LINE) USING OFF-RESONANCE TRANSFER	12
FIGURE 6: TABLE OF VALUES OF FIELD STRENGTH AND DURATION FOR OPTIMAL STCP TRANSFER	13
FIGURE 7: LIOUVILLIAN EIGENFREQUENCY ($1=1 \times J$) DEPENDENCE OF w (Ω_{TOT}/J RATIO)	15
FIGURE 8: PULSE SEQUENCE FOR SINGLE TRANSITION SEPARATING COHERENCE TRANSFER	17
FIGURE 9: PULSE SEQUENCE FOR CREATION OF SINGLE TRANSITION COHERENCE	19
FIGURE 10: PULSE SEQUENCE FOR CREATION OF SINGLE TRANSITION COHERENCE ELIMINATING LONGITUDINAL MAGNETISATION	20
FIGURE 11: PULSE SEQUENCE USED IN EXPERIMENTS	21
FIGURE 12: SIMULATED EVOLUTION OF ON-RESONANCE STCP TRANSFER NEGLECTING RELAXATION	22
FIGURE 13: SIMULATED EVOLUTION OF OFF-RESONANCE STCP TRANSFER NEGLECTING RELAXATION	22
FIGURE 14: MEASURED EVOLUTION OF ON-RESONANCE STCP TRANSFER IN TBOC-GLYCINE	23
FIGURE 15: MEASURED EVOLUTION OF OFF-RESONANCE STCP TRANSFER IN TBOC-GLYCINE	23
FIGURE 16: MEASURED PROTON PEAK INTENSITY AS A FUNCTION OF DELAY BEFORE DETECTION	24
FIGURE 17: CALCULATED MAGNITUDE SPECTRUM OF EXPONENTIAL DECAY WITH 9.7 MS RELAXATION TIME	25
FIGURE 18: SIMULATED EVOLUTION OF ON-RESONANCE STCP TRANSFER IN SUCROSE	26
FIGURE 19: SIMULATED EVOLUTION OF OFF-RESONANCE STCP TRANSFER IN SUCROSE	27
FIGURE 20: MEASURED EVOLUTION OF ON-RESONANCE STCP TRANSFER IN SUCROSE	27
FIGURE 21: MEASURED EVOLUTION OF OFF-RESONANCE STCP TRANSFER IN SUCROSE	28

Abbreviations

CP	Cross Polarisation
CPMG	Carr-Purcell-Meiboom-Gill experiment for transverse relaxation rate measurement
HH	Hartmann-Hahn
HSQC	Heteronuclear Single Quantum Coherence spectroscopy
INEPT	Insensitive Nuclei Enhancement by Polarisation Transfer
LvN equation	Liouville-von Neumann equation
NMR	Nuclear Magnetic Resonance
RF	Radio Frequency
ST	Single Transition
STCP	Single Transition Cross Polarisation
TROSY	Transverse Relaxation Optimised Spectroscopy

Symbols

\in	Denotes that an element belongs to a set, e.g. $\Psi \in \mathbf{L}$, usually implying it has certain properties.
$[\]^*$	Complex conjugate
$[\]^{-1}$	Inverse of scalar, operator or super operator
$\{ \dots \}$	A set consisting of the elements within the brackets
\Leftrightarrow	Denotes equivalence, e.g. $(A=B) \Leftrightarrow (B=A)$
\Rightarrow	Denotes deduction, e.g. $(A>B, B>C) \Rightarrow (A>C)$
$[\hat{A}, \hat{B}]$	Commutator between \hat{A} and \hat{B} : $[\hat{A}, \hat{B}] = \hat{A}\hat{B} - \hat{B}\hat{A}$
$tr\{\hat{A}\}$	Trace of operator \hat{A}
$\langle \Psi \Phi \rangle$	Inner product of Ψ and Φ
$ \Psi\rangle\langle\Phi $	Outer product of Ψ and Φ
\hat{A}	Arbitrary operator
Ψ	Arbitrary wave function
\vec{I}	Explicit vector representation
$[G]$	Explicit matrix representation
J	The scalar coupling constant (Hz)
τ	Inverse scalar coupling constant = $1/J$ (s)
Ω	Irradiation field strength (Hz)
w	Combined irradiation field – J-coupling ratio = Ω_{tot}/J (unitless)
T_2	Transverse relaxation time (s)
$\hat{\sigma}$	Spin system density operator
\hat{H}	Hamiltonian operator (Hz)
$\hat{\hat{H}}$	Hamiltonian super operator (Hz)
$\hat{\hat{R}}$	Relaxation super operator (Hz)
$\hat{\hat{\Gamma}}$	Liouvillian super operator = $i\hat{\hat{H}} - \hat{\hat{R}}$ (Hz)
α, β	Spin function eigenstates
λ_i	Operator eigenvalue, indexed by i
κ_{ij}	Super operator eigenvalue, double indexed by i and j by reasons of convenience
\in_{ij}	Unitary second rank tensor: $\in_{ij} = (1 \text{ if } i=j, 0 \text{ otherwise})$

Index

C	
commutation rules.....	3
commutator.....	4
conclusions.....	28
conventional cross polarisation.....	7
D	
density operator.....	2
E	
eigenfunction.....	1
eigenvalue.....	1
requirements for optimal transfer.....	12
ensemble.....	2
expectation values.....	1
experiments	
general experimental aspects.....	17
on sucrose.....	26
on tboc-glycine.....	21
G	
Gamma subroutine package.....	20
gradients.....	17
H	
Hamiltonian.....	2, 10
eigenfrequency theory.....	12
super operator.....	4
time independent.....	9
transfer Hamiltonian	
eigenfrequencies.....	13
matrix representation.....	13
Hartman-Hahn condition.....	7, 8
I	
INEPT pulse sequence.....	8
L	
Liouville space.....	3
Liouville-von Neumann equation.....	4
Liouvillian	
transfer Liouvillian	
eigenfrequencies.....	13
Liouvillian	
eigenfrequency theory.....	12
liquid state cross polarisation.....	7
M	
master equation.....	5
solving.....	5
O	
operator.....	1
optimal transfer	
Irradiation duration.....	15
transfer field strength.....	14
P	
peak broadening compensation.....	23
R	
relaxation super operator.....	5
requirements on STCP.....	10
S	
Schrödinger equation.....	2, 4
simulation	
including relaxation.....	25
neglecting relaxation.....	20
single transition coherences	
creation.....	18
operators.....	3
solid state cross polarisation.....	7
T	
transfer field	
matching.....	17
transverse relaxation measurement.....	23
W	
water suppression.....	17
wave function.....	1